

# Has J-PARC E07 observed a $\Xi_{1s}^-$ nuclear state?

E. Friedman, A. Gal

*Racah Institute of Physics, The Hebrew University, 9190401 Jerusalem, Israel*

---

## Abstract

The Strangeness  $\mathcal{S} = -2$  J-PARC E07 emulsion experiment published recently two new  $\Xi^-$ - $^{14}\text{N}$  capture events, IRRAWADDY and IBUKI, identified by observing weak-decay sequences of pairs of single- $\Lambda$  hypernuclei and interpreted as  $\Xi_{1s}^-$  and  $\Xi_{1p}^-$  nuclear bound states, respectively, with binding energies  $B_{\Xi_{1s}^-}^{1s} = 6.27 \pm 0.27$  MeV and  $B_{\Xi_{1p}^-}^{1p} = 1.27 \pm 0.21$  MeV.  $\Xi^-$  capture events in emulsion play a major role in determining the  $\Xi$ -nuclear and the  $\Lambda\Lambda$  potential strengths. Here we question the assignment of a  $\Xi_{1s}^-$  nuclear bound state to IRRAWADDY and offer an alternative assignment as a near-threshold  $\Xi_{1p}^0$ - $^{14}\text{C}$  nuclear bound state, slightly admixed with a  $\Xi_{1p}^-$ - $^{14}\text{N}$  nuclear bound state component corresponding to IBUKI. We also question using IBUKI's  $B_{\Xi_{1p}^-}^{1p}$  value as is to determine the  $\Xi$ -nuclear potential depth. Altogether,  $\Xi^-$  capture events in  $^{12}\text{C}$  and  $^{16}\text{O}$  should prove less ambiguous than in  $^{14}\text{N}$ .

*Keywords:*  $\Xi$  nuclear bound states.

---

## 1. Introduction

Experimental input to deciphering the Strangeness  $\mathcal{S} = -2$  sector of hypernuclear physics comes mostly from forming  $\Xi^-$  hyperons by a  $(K^-, K^+)$  reaction on nuclear targets and stopping them in light-nuclei emulsion [1]. Data collected in the last 30 years by KEK emulsion experiments E176 [2] and E373 [3, 4] have advanced our understanding of  $\Lambda\Lambda$  and  $\Xi N$  nuclear dynamics [5]. New J-PARC E07  $\Xi^-$  capture data, some of which were presented recently [6, 7, 8], may advance it further.

Because of the large momentum transfer in the  $(K^-, K^+)$  nuclear reaction which converts protons to  $\Xi^-$  hyperons, only very few of the produced high-energy  $\Xi^-$  hyperons slow down sufficiently in the surrounding nuclear emulsion to undergo Auger process, form high- $n$  atomic state, and cascade

down radiatively. In light-nuclei emulsion, strong-interaction  $\Xi^- p \rightarrow \Lambda\Lambda$  capture takes over radiative cascade beginning at a  $3D$  atomic state bound by 126, 175, 231 keV in C, N, O, respectively, although the  $3D$  strong-interaction shift is still small, less than 1 keV [9]. Capture events are recorded by observing  $\Lambda$  hyperons or  $\Lambda$ -hypernuclear decay products. Interestingly, several observed decay sequences of twin (pairs of) single- $\Lambda$  hypernuclei were found to follow capture from a lower  $\Xi^-$  orbit, namely Coulomb-assisted  $1p_{\Xi^-}$  nuclear states in  $^{12}\text{C}$  and  $^{14}\text{N}$  [2, 4, 7].

Table 1: Reported two-body  $\Xi^-$  capture events in  $^{14}\text{N}$ ,  $\Xi^- + ^{14}\text{N} \rightarrow ^{A'}_{\Lambda}Z' + ^{A''}_{\Lambda}Z''$ , to twin  $\Lambda$  hypernuclei, some in ground states, some in specific excited states marked by asterisk. Of these, only IBUKI is uniquely assigned. Fitted  $\Xi^-$  binding energies  $B_{\Xi^-}^{1p}$  are listed.

Experiment	Event	$^{A'}_{\Lambda}Z' + ^{A''}_{\Lambda}Z''$	$B_{\Xi^-}^{1p}$ (MeV)
KEK E176 [2]	14-03-35	$^3_{\Lambda}\text{H} + ^{12}_{\Lambda}\text{B}$	$1.18 \pm 0.22$
KEK E373 [4]	KISO	$^5_{\Lambda}\text{He} + ^{10}_{\Lambda}\text{Be}^*$	$1.03 \pm 0.18$
J-PARC E07 [7]	IBUKI	$^5_{\Lambda}\text{He} + ^{10}_{\Lambda}\text{Be}$	$1.27 \pm 0.21$

The J-PARC light-nuclei emulsion experiment E07 reported two  $\Xi^-$  capture events in  $^{14}\text{N}$ , uniquely identified by their subsequent single- $\Lambda$  hypernuclear decay sequences, and with sufficiently small binding-energy uncertainty (say  $\lesssim 0.3$  MeV) to become potentially informative. One event, named IBUKI, was assigned as a  $\Xi^-_{1p}$ - $^{14}\text{N}$  bound state, with binding energy  $B_{\Xi^-}$  listed in Table 1 together with similar  $B_{\Xi^-}$  values for  $\Xi^-$ - $^{14}\text{N}$  capture events found in KEK experiments E176 and E373. All three listed  $B_{\Xi^-}$  values are slightly above 1 MeV, significantly higher than the purely-Coulomb  $2P$  atomic binding energy value of about 0.4 MeV in  $^{14}\text{N}$ , thereby corresponding to a Coulomb-assisted  $1p_{\Xi^-}$  nuclear state in  $^{14}\text{N}$  that evolves from a  $2P$  atomic state. Unfortunately, it is just one of five  $\Xi^-_{1p}$ - $^{14}\text{N}_{\text{g.s.}}$  configuration states spread over  $\sim 1.3$  MeV (see Appendix to the present work) which makes IBUKI unfit to constrain reliably the  $\Xi$ -nuclear potential strength [10].

The other event, with binding energy  $B_{\Xi^-} = 6.27 \pm 0.27$  MeV, was named IRRAWADDY and assigned as a  $\Xi^-_{1s}$  nuclear state [8]. Both IBUKI and IRRAWADDY are shown on the r.h.s. of Fig. 1, fed by radiative E1 transitions from the upper  $3D$   $\Xi^-$ -atom state. Another  $\Xi^-_{1s}$  candidate event KINKA, with two possible  $B_{\Xi^-}$  values of  $8.00 \pm 0.77$  and  $4.96 \pm 0.77$  MeV, was deduced by revisiting KEK-E373 capture events [8]. A KINKA+IRRAWADDY

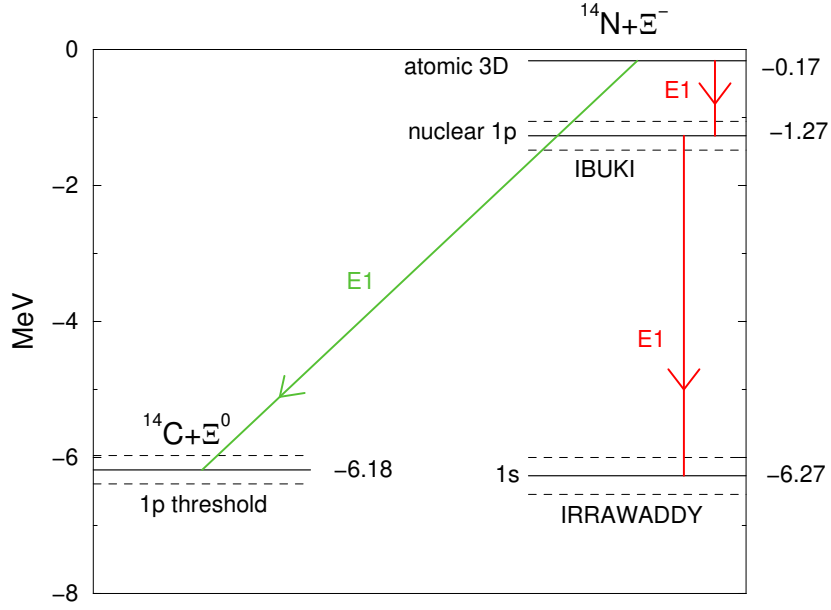


Figure 1: Level diagram of  $\Xi^- + {}^{14}\text{N}$ . Shown on the right are a  $3D$  atomic state and  $1p, 1s$  nuclear states assigned, respectively, to E07  $\Xi^-$  capture events IBUKI and IRRAWADDY [7, 8]. The  $\Xi^0 + {}^{14}\text{C}$  threshold at  $-6.18$  MeV is marked on the left. Electromagnetic  $E1$  transitions deexciting the  $\Xi_{3D}^-$  atomic state to lower  $\Xi^- - {}^{14}\text{N}$  and  $\Xi_{1p}^- - {}^{14}\text{C}$  nuclear states from which  $\Xi$  hyperon capture may occur are marked by red and green arrowed lines, respectively. A near-threshold  $\Xi_{1p}^0 - {}^{14}\text{C}$  state on the left provides an alternative interpretation of IRRAWADDY.

weighted average of  $B_{\Xi^-} = 6.13 \pm 0.25$  or  $6.46 \pm 0.25$  MeV, differs little from IRRAWADDY's own value of  $B_{\Xi^-} = 6.27 \pm 0.27$  MeV.

We note that  $2P \rightarrow 1S$  radiative decay rates are of order 1% of  $3D \rightarrow 2P$  radiative decay rates [11, 12] suggesting that  $\Xi^-$  capture from a nuclear  $\Xi_{1s}^- - {}^{14}\text{N}$  state is suppressed to this order relative to capture from a nuclear  $\Xi_{1p}^- - {}^{14}\text{N}$  state. Assigning a  $\Xi_{1s}^- - {}^{14}\text{N}$  bound state to IRRAWADDY is therefore questionable. Here we explore an alternative assignment, as follows.

Little attention if any was given to mixing between  $\Xi^-$  states in  ${}^{14}\text{N}$  and  $\Xi^0$  states in  ${}^{14}\text{C}$ , induced by the  $\Xi^- p \leftrightarrow \Xi^0 n$  strong-interaction charge exchange. Nuclear ground-state mass differences for  $Z \rightarrow (Z - 1)$  isobars in the main light-nuclei emulsion elements  ${}^{12}\text{C}$ ,  ${}^{14}\text{N}$  and  ${}^{16}\text{O}$  are listed in Table 2. Note that the nuclear mass difference  $M({}^{14}\text{C}) - M({}^{14}\text{N})$  is smaller than the  $\Xi$  hyperon mass difference  $m_{\Xi^-} - m_{\Xi^0} = 6.85 \pm 0.21$  MeV [14].

This means that  $\Xi^0-^{14}\text{C}$  bound states, if and when exist, lie always below the  $\Xi^{-}-^{14}\text{N}$  threshold. To be more precise, the  $\Xi^0-^{14}\text{C}$  threshold for a virtual  $^{14}\text{N}(\Xi^-, \Xi^0)^{14}\text{C}$  charge-exchange reaction is at  $\Xi^{-}-^{14}\text{N}$  energy of

$$-(6.85 \pm 0.21) + 0.67 = -(6.18 \pm 0.21) \text{ MeV}. \quad (1)$$

Remarkably, the  $\Xi^0-^{14}\text{C}$  threshold energy in  $\Xi^{-}-^{14}\text{N}$ , Eq. (1), is within the reported IRRAWADDY bound-state energy interval  $-(6.27 \pm 0.27)$  MeV, as shown in Fig. 1.

Table 2: Ground-state nuclear mass differences (in MeV) for  $Z \rightarrow Z - 1$  isobars of the main light-nuclei emulsion elements  $^{12}\text{C}$ ,  $^{14}\text{N}$  and  $^{16}\text{O}$  [13].

$M(^{12}\text{B})-M(^{12}\text{C})$	$M(^{14}\text{C})-M(^{14}\text{N})$	$M(^{16}\text{N})-M(^{16}\text{O})$
13.88	0.67	10.93

The aim of the present note is to show that this remarkable coincidence may not be accidental, and that IRRAWADDY is likely to stand for a near-threshold  $\Xi_{1p}^0-^{14}\text{C}$  bound state that has nothing to do with a  $\Xi_{1s}^{-}-^{14}\text{N}$  bound state suggested by E07. To do so, we first discuss in Sect. 2 conditions for a near-threshold  $\Xi_{1p}^0-^{14}\text{C}$  bound state using a  $\Xi$ -nuclear potential constrained by our recent work [10] on  $\Xi_{1p}^{-}-^{12}\text{C}$  capture events. We then evaluate in Sect. 3 the mixing induced by the  $\Xi N$  strong interaction between a  $\Xi_{1p}^{-}-^{14}\text{N}$  bound state identified with J-PARC E07 IBUKI and a  $\Xi_{1p}^0-^{14}\text{C}$  bound state lying about 5 MeV below IBUKI, within the J-PARC E07 experimental uncertainty of IRRAWADDY. Provided such mixing is not prohibitively small,  $E1$  radiative deexcitation of the  $\Xi_{3D}^{-}-^{14}\text{N}$  atomic state occurs to *both*  $\Xi_{1p}^{-}-^{14}\text{N}$  and  $\Xi_{1p}^0-^{14}\text{C}$  nuclear states, as verified in Sect. 3. Discussion and summary follow in Sect. 4 and a brief Appendix describes the  $\Xi_{1p}^{-}-^{14}\text{N}_{g.s.}$  configuration.

## 2. $\Xi_{1p}^0-^{14}\text{C}$ binding

Following the optical model methodology introduced in our recent work on low-energy  $\Xi^{-}$ -nuclear interactions [10], the strong-interaction optical potential used here is of the form

$$V_{\text{opt}}^{\Xi}(r) = -\frac{2\pi}{\mu} \left(1 + \frac{A-1}{A} \frac{\mu}{m_N}\right) [b_0(\rho) \rho(r) + b_1 \rho_{\text{exc}}(r)]. \quad (2)$$

Here  $\mu$  is the  $\Xi^-$ -nuclear reduced mass, and  $b_0$  and  $b_1$  are effective  $\Xi N$  c.m. scattering amplitudes related to the isoscalar  $V_0$  and isovector  $V_\tau$  components, respectively, of the two-body  $s$ -wave  $\Xi N$  interaction  $V_{\Xi N}$ ,

$$V_{\Xi N} = V_0 + V_\sigma \vec{\sigma}_\Xi \cdot \vec{\sigma}_N + V_\tau \vec{\tau}_\Xi \cdot \vec{\tau}_N + V_{\sigma\tau} \vec{\sigma}_\Xi \cdot \vec{\sigma}_N \vec{\tau}_\Xi \cdot \vec{\tau}_N, \quad (3)$$

with  $V$ s functions of  $r_{\Xi N}$ . The density  $\rho = \rho_n + \rho_p$  in Eq. (2) is a nuclear density distribution normalized to  $A$ , and  $\rho_{\text{exc}} = \rho_n - \rho_p$  is a neutron-excess density with  $\rho_n = (N/Z)\rho_p$ , implying that  $\rho_{\text{exc}} = 0$  for the  $N = Z$  emulsion nuclei  $^{12}\text{C}$ ,  $^{14}\text{N}$  and  $^{16}\text{O}$ . The r.m.s. radius of  $\rho_p$  was set equal to that of known nuclear charge densities, as discussed in our earlier work [10]. Finally, the density-dependent  $b_0(\rho)$  is given by

$$b_0(\rho) = \frac{\text{Re } b_0}{1 + \frac{3k_F}{2\pi} \text{Re } b_0^{\text{lab}}} + \text{Im } b_0, \quad k_F = (3\pi^2 \rho/2)^{\frac{1}{3}}, \quad (4)$$

with Fermi momentum  $k_F$  and  $b_0^{\text{lab}} = (1 + \frac{m_{\Xi^-}}{m_N})b_0$ . Eq. (4) accounts for Pauli correlations in  $\Xi N$  in-medium multiple scatterings [15]. The value of  $\text{Im } b_0$  is fixed at 0.01 fm to simulate  $\Xi N \rightarrow \Lambda\Lambda$  conversion.

Using  $b_0 = (0.527 + i0.010)$  fm from fitting  $B_{\Xi^-}^{1p} = 0.82$  MeV in  $^{12}\text{C}$  [10], together with  $b_1 = 0$ , failed to produce a  $\Xi_{1p}^0$ - $^{14}\text{C}$  bound state. This agrees with  $\Xi_{1p}^-$ - $^{12}\text{C}$  being a Coulomb-assisted bound state, unbound without the  $\Xi^-$ -nuclear Coulomb potential  $V_C$ . However, a likely source of additional attraction for  $\Xi_{1p}^0$ - $^{14}\text{C}$ , with  $N \neq Z$ , is provided by the  $\Xi N$  strong-interaction  $V_\tau$  isovector component in terms of  $b_1 \neq 0$ . Indeed, varying  $b_1$  between 0.270 to 0.420 fm produces  $\Xi_{1p}^0$  binding energies in  $^{14}\text{C}$  ranging between  $-200$  to 178 keV, comfortably within IRRAWADDY's binding energy uncertainty, and widths between 274 to 409 keV.<sup>1</sup> These  $b_1$  values, relative to  $b_0$ , are of the same sign and order of magnitude expected from the HAL-QCD lattice derivation of  $V_{\Xi N}$  [17] and from the chiral EFT calculation at NLO of  $\Xi$  in nuclear matter [18]. The corresponding  $\Xi_{1p}^0$  radial wavefunctions reach a maximum value between 2.66 to 2.54 fm in the 378 keV binding energy interval specified above. Furthermore, the  $\Xi_{1p}^-$ - $^{14}\text{N}$  Coulomb-assisted bound state wavefunction generated for the same value of  $b_0$ , but  $b_1 = 0$  as appropriate to the  $T = 0$   $^{14}\text{N}$ , reaches its maximum at 2.62 fm, overlapping to better than 0.98 with any of the  $\Xi_{1p}^0$ - $^{14}\text{C}$  wavefunctions in the range considered above.

---

<sup>1</sup>Normalizable  $1p$  bound states above the  $\Xi^0$ - $^{14}\text{C}$  threshold are generated owing to the imaginary part of  $V_{\text{opt}}^\Xi$  in Eq. (2), see Ref. [16] for discussion of  $\Sigma$  nuclear states above threshold.

### 3. $\Xi_{1p}^0 -^{14}\text{C} \leftrightarrow \Xi_{1p}^- -^{14}\text{N}$ mixing

To evaluate the  $\Xi_{1p}^- -^{14}\text{N}$  to  $\Xi_{1p}^0 -^{14}\text{C}$  mixing amplitude we use realistic shell-model wavefunctions for  $^{14}\text{N}_{\text{g.s.}}$  and  $^{14}\text{C}_{\text{g.s.}}$  [19]:

$$|^{14}\text{C}(J^\pi = 0^+; T = 1)\rangle = 0.7729\ ^1S + 0.6346\ ^3P, \quad (5)$$

$$|^{14}\text{N}(J^\pi = 1^+; T = 0)\rangle = 0.1139\ ^3S + 0.2405\ ^1P + 0.9639\ ^3D, \quad (6)$$

where the  $^{2S+1}L$  spin-orbital basis wavefunctions refer to the two-hole  $(1p_N)^{-2}$  configuration in the nuclear  $p$ -shell. A check on the  $S$  and  $P$  amplitudes is provided by the near vanishing of the weak-interaction Gamow-Teller (GT)  $\Delta S = \Delta T = 1$  matrix element  $\langle ^{14}\text{N}(1^+; 0) | \sum \vec{\sigma}_i \tau_i^+ | ^{14}\text{C}(0^+; 1) \rangle$  responsible for the extremely long lifetime of  $^{14}\text{C}_{\text{g.s.}}(0^+; 1)$  in its  $\beta$ -decay to  $^{14}\text{N}_{\text{g.s.}}(1^+; 0)$ . The near vanishing of this GT matrix element occurs owing to a strong cancelation between the  $\Delta L = 0$   $^3S_1 \leftrightarrow ^1S_0$  and  $^1P_1 \leftrightarrow ^3P_0$  GT transitions, persisting also for the same  $\Delta L = 0$  transitions induced by the  $V_{\sigma\tau} \vec{\sigma}_\Xi \cdot \vec{\sigma}_N \vec{\tau}_\Xi \cdot \vec{\tau}_N$  term of the strong-interaction  $V_{\Xi N}$ , Eq. (3), in mixing  $\Xi_{1s}^- -^{14}\text{N}(1^+; 0)$  with  $\Xi_{1s}^0 -^{14}\text{C}(0^+; 1)$ . However, the  $\Xi_{1p}^- -^{14}\text{N}(1^+; 0)$  to  $\Xi_{1p}^0 -^{14}\text{C}(0^+; 1)$  mixing is governed by a normal-strength  $\Delta L = 2$  matrix element that couples the dominant  $^3D_1$  amplitude in  $^{14}\text{N}_{\text{g.s.}}(1^+; 0)$  to the  $^1S_0$  and  $^3P_0$  amplitudes in  $^{14}\text{C}_{\text{g.s.}}(0^+; 1)$ .

Table 3: Coefficients of  $F_{\Xi N}^{(2)}(V_{\sigma\tau})$  in mixing matrix elements between two  $J^\pi = \frac{1}{2}^-$  states:  $\Xi_{1p}^0 -^{14}\text{C}(0^+; 1)$  and the  $\Xi_{1p}^- -^{14}\text{N}(1^+; 0)$  IBUKI state. Entries are labeled by  $^{2S+1}L$  components of  $A = 14$  wavefunctions given by Eqs. (5) and (6).

	$^{2S+1}L$	$^3S$	$^1P$	$^3D$
$^1S$		–	–	$\frac{4\sqrt{2}}{5\sqrt{5}}$
$^3P$		–	$\frac{2\sqrt{2}}{5\sqrt{3}}$	$\frac{6}{5\sqrt{5}}$

The IBUKI state, as detailed in the Appendix, is a  $J^\pi = \frac{1}{2}^-$  state built by coupling a  $s_{\Xi^-} = \frac{1}{2}$  Pauli-spin to  $\Lambda^\pi = 0^-$ , where  $\vec{\Lambda} = \vec{J}_N + \vec{\ell}_\Xi$ . The full  $\Xi_{1p}^- -^{14}\text{N}(1^+; 0)$  configuration includes also  $\Lambda^\pi = 1^-, 2^-$  states. As for the  $\Xi_{1p}^0 -^{14}\text{C}(0^+; 1)$  configuration, it consists of a  $J^\pi = (\frac{1}{2}^-, \frac{3}{2}^-)$  spin-orbit doublet obtained by coupling  $s_{\Xi^0} = \frac{1}{2}$  to the only possible  $\Lambda^\pi = 1^-$  state. Mixing matrix elements of  $V_{\sigma\tau} \vec{\sigma}_\Xi \cdot \vec{\sigma}_N \vec{\tau}_\Xi \cdot \vec{\tau}_N$  between these  $J^\pi = \frac{1}{2}^-$  states are listed in Table 3 in terms of  $LS$  basis components of the  $^{14}\text{C}(0^+; 1)$  and  $^{14}\text{N}(1^+; 0)$

ground-state wavefunctions, Eqs. (5) and (6). These matrix elements need to be multiplied by the corresponding Slater integral  $F_{\Xi N}^{(2)}(V_{\sigma\tau})$ .

Using Eqs. (5) and (6) for the nuclear  $LS$  basis amplitudes and the  $LS$  matrix elements listed in Table 3, one gets the mixing matrix element between the  $J^\pi = \frac{1}{2}^-$  relevant  $\Xi_{1p}^0-^{14}\text{C}_{\text{g.s.}}$  and  $\Xi_{1p}^- -^{14}\text{N}_{\text{g.s.}}$  states in terms of  $F_{\Xi N}^{(2)}(V_{\sigma\tau})$ :

$$\langle \Xi_{1p}^0 -^{14}\text{C}_{\text{g.s.}} | V_{\sigma\tau} \vec{\sigma}_{\Xi} \cdot \vec{\sigma}_N \vec{\tau}_{\Xi} \cdot \vec{\tau}_N | \Xi_{1p}^- -^{14}\text{N}_{\text{g.s.}} \rangle = (0.705 + 0.050) F_{\Xi N}^{(2)}(V_{\sigma\tau}). \quad (7)$$

Here the two matrix elements involving the dominant  ${}^3D$  component in  ${}^{14}\text{N}(1^+; 0)$  contribute coherently to give most of the mixing,  $0.705F^{(2)}$ , and the contribution of the  $P$ -states mixing,  $0.050F^{(2)}$ , is small on this scale. For a conservative estimate we take  $F_{\Xi N}^{(2)}(V_{\sigma\tau}) \approx -0.6$  MeV, which is 20% of the value of  $F_{\Xi N}^{(2)}(V_0)$  used in Ref [10] to reproduce IBUKI, thereby getting  $\approx -0.453$  MeV for the overall mixing matrix element. The resulting amplitude of IBUKI's admixture into  $\Xi_{1p}^0-^{14}\text{C}_{\text{g.s.}}$ , now identified with IRRAWADDY, is obtained upon dividing it by  $\Delta E_{1p} \approx 5$  MeV for the energy difference between the two admixed  $1p_{\Xi}$  nuclear states:  $-0.453/5 = -0.0906$ , and  $0.00821$  upon squaring it. The radiative  $E1$  transition rate from  $3D_{\Xi^-}$  to  $1p_{\Xi}$  states through their  $\Xi_{1p}^- -^{14}\text{N}_{\text{g.s.}}$  components goes like  $(\Delta E)^3$ , with a large factor of  $(6.1/1.1)^3 \approx 171$  in favor of populating the lower,  $\Xi_{1p}^0-^{14}\text{C}_{\text{g.s.}}$  state. Altogether one gets a ratio of  $0.00821 \times 171 = 1.40$  between the two  $E1$  rates, making them roughly equal to each other. A schematic plot of these two  $E1$  transitions is shown in Fig. 1.

#### 4. Discussion and summary

Before summarizing it is appropriate to discuss briefly the role played by the choice of  $\Xi^-$  capture data input in predicting  $\Xi$ -nuclear bound states and potential depths. In our recent work [10] two KEK-E176  ${}^{12}\text{C}$  events [2] with  $B_{\Xi^-}^{1p}({}^{12}\text{C}) = 0.82 \pm 0.14$  MeV served as input for setting up the  $\Xi$ -nuclear optical potential depth at nuclear-matter density,  $-V_{\Xi}(\rho_0) = 21.9 \pm 0.7$  MeV, and for explaining IBUKI's  $B_{\Xi^-}^{1p}({}^{14}\text{N}) = 1.27 \pm 0.21$  MeV (see Appendix). Predicting  $B_{\Xi^-}^{1s}$  values from a  $B_{\Xi^-}^{1p}$  input value requires introduction of a more systematic density dependence, as done in  $\Lambda$  hypernuclear studies [21]. Choosing alternatively the J-PARC E07  ${}^{14}\text{N}$  IRRAWADDY event [8] as input, with  $B_{\Xi^-}^{1s}({}^{14}\text{N}) = 6.27 \pm 0.27$  MeV, gives rise to predictions listed in Table 4. Among the  $\Xi_{1p}^-$  bound states listed in the table, the  $\Xi_{1p}^- -^{12}\text{C}$  binding energy comes out exceedingly small compared to that determined from the KEK E176 [2]

capture events.<sup>2</sup> We note that a 13.8 MeV potential depth value listed in the table agrees closely with the depth derived in a recent Skyrme-Hartree-Fock calculation [23] that focuses on the  $^{14}\text{N}$  KINKA and IBUKI capture events.

Table 4:  $\Xi^- - ^{12}\text{C}$  and  $\Xi^- - ^{14}\text{N}$  binding energies (MeV) in  $1s$  and  $1p$  states, plus the  $\Xi$  nuclear potential depth (MeV) at nuclear-matter density  $\rho_0 = 0.17 \text{ fm}^{-3}$ , calculated using a density-dependent optical potential Eqs. (2,4) with  $\text{Re } b_0$  fitted to the  $\Xi^- - ^{14}\text{N}$   $1s$  binding energy assigned by J-PARC E07 [8] to IRRAWADDY as underlined here.

Input	$\Xi_{1s}^- - ^{12}\text{C}$	$\Xi_{1p}^- - ^{12}\text{C}$	$\Xi_{1s}^- - ^{14}\text{N}$	$\Xi_{1p}^- - ^{14}\text{N}$	$-V_{\Xi}(\rho_0)$
IRRAWADDY	4.94	0.32	<u>6.27</u>	0.50	13.8

The solution offered here to the difficulty of interpreting IRRAWADDY as a  $\Xi_{1s}^-$  bound state in  $^{14}\text{N}$  is by pointing out that it could correspond to a  $\Xi_{1p}^0 - ^{14}\text{C}$  bound state, something that cannot happen kinematically in the other light-emulsion nuclei  $^{12}\text{C}$  and  $^{16}\text{O}$ . We showed in the present work that radiative  $E1$  deexcitation of the  $\Xi^- - ^{14}\text{N}$  atom, proceeding through the  $\Xi_{3D}^-$  atomic state, leads at comparable rates to two  $\Xi_{1p}$ -nuclear states coupled by  $\Xi^- p \leftrightarrow \Xi^0 n$  strong-interaction charge exchange. One state, of dominantly  $\Xi_{1p}^- - ^{14}\text{N}$  structure is the one assigned commonly to IBUKI, and the other one, of dominantly  $\Xi_{1p}^0 - ^{14}\text{C}$  structure is assigned here to IRRAWADDY. The latter assignment contrasts with viewing IRRAWADDY as a  $\Xi_{1s}^- - ^{14}\text{N}$  state, an assignment motivated only by its binding energy of a few MeV. Given that in this nuclear mass range capture rates from  $1s_{\Xi^-}$  states are estimated to be two orders of magnitude below capture rates from  $1p_{\Xi^-}$  states [11, 12], this  $\Xi_{1p}^0 - ^{14}\text{C}$  new assignment addresses satisfactorily the capture rate hierarchy. Establishing  $1s_{\Xi^-}$  states in light emulsion nuclei requires focusing on capture events in  $^{12}\text{C}$  and  $^{16}\text{O}$ , where the  $\Xi^- p \leftrightarrow \Xi^0 n$  coupling is ineffective.

<sup>2</sup>Regarding  $\Xi_{1p}^- - ^{12}\text{C}$ , the density-folded  $G$ -matrix Ehime potential calculation of Ref. [22], using an outdated value  $B_{\Xi_{1p}^-}^{1p}(^{12}\text{C})=0.58$  MeV for input, nearly reproduced IRRAWADDY and IBUKI long time before their observation. Recalling, however, that 0.58 MeV is almost half the way from the KEK E176 reported value 0.82 MeV [2] down to the pure-Coulomb value  $B_{\Xi_{1p}^-}^{2P}(^{12}\text{C})=0.28$  MeV, their results require revision. Furthermore, since  $J(^{14}\text{N}) \neq 0$  (see Appendix) their calculated  $B_{\Xi_{1p}^-}^{1p}(^{14}\text{N})$  value cannot be compared directly with IBUKI's binding energy of  $1.27 \pm 0.27$  MeV in  $^{14}\text{N}$  [7].

## Appendix A. $\Xi_{1p}^-$ spectrum in $^{14}\text{N}$

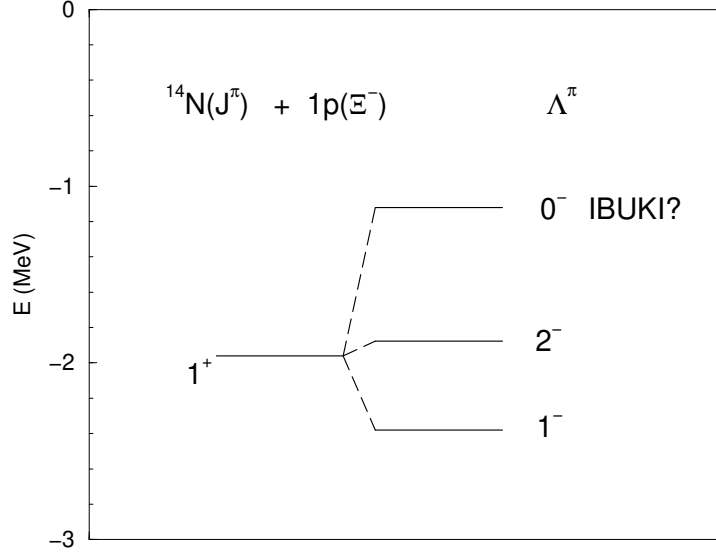


Figure A.1: Spectrum of  $^{14}\text{N}_{\text{g.s.}} + 1p_{\Xi^-}$  states labeled by  $\Lambda^\pi$ , see text. Figure revising Fig. 2 in Ref. [10].

The  $\Xi_{1p}^- - ^{14}\text{N}(1^+; 0)$  configuration consists of two  $J^\pi = \frac{1}{2}^-$  states, two  $J^\pi = \frac{3}{2}^-$  states and one  $J^\pi = \frac{5}{2}^-$  state obtained by coupling  $s_{\Xi^-} = \frac{1}{2}$  Pauli-spin to  $\vec{\Lambda} = \vec{J}_N + \vec{\ell}_{\Xi^-}$ . Here  $J_N^\pi = 1^+$ ,  $\ell_{\Xi^-}^\pi = 1^-$ , so that  $\Lambda^\pi = 0^-, 1^-, 2^-$  as shown in Fig. A.1. The energy splittings marked in the figure follow from a shell-model quadrupole-quadrupole spin-independent residual interaction  $\mathcal{V}_{\Xi N}^Q$ ,

$$\mathcal{V}_{\Xi N}^Q = F_{\Xi N}^{(2)} Q_N \cdot Q_{\Xi}, \quad Q_B = \sqrt{\frac{4\pi}{5}} Y_2(\hat{r}_B), \quad (\text{A.1})$$

where  $F^{(2)}$  is the corresponding Slater integral. For more details see Ref. [10] where it was also argued that the dependence on  $s_{\Xi^-}$  is secondary to the dependence on  $\Lambda$ . The  $(2\Lambda + 1)$ -averaged energy  $-1.96 \pm 0.26$  MeV was calculated using a central optical potential  $V_{\text{opt}}^\Xi$  specified in Sect. 2, with  $b_0$  fitted to KEK-E176  $\Xi^- - ^{12}\text{C}$  capture events [10]. The energy  $E = -1.12$  MeV of the  $\Lambda^\pi = 0^-$  state is close to the energy  $E \approx -1.16$  MeV deduced from the  $\Xi^- - ^{14}\text{N}$  capture events listed in Table 1. Thus, the IBUKI state corresponds

to a unique  $J^\pi = \frac{1}{2}^-$  state built on  $\Lambda^\pi = 0^-$ , the highest in the  $\Lambda$  spectrum shown in the figure. To the best of our knowledge, this has not been realized in any past calculation of the  $\Xi_{1p}^- -^{14}\text{N}(1^+; 0)$  spectrum.

## Acknowledgments

We thank Dr. K. Nakazawa for useful correspondence with one of us (A.G.) following his talk at HYP2022. This work was supported by the European Union's Horizon 2020 research and innovation programme under grant agreement No. 824093.

## References

- [1] E. Hiyama, K. Nakazawa, *Annu. Rev. Nucl. Part. Sci.* 68 (2018) 131.
- [2] S. Aoki, et al., KEK E176 Collaboration, *Nucl. Phys. A* 828 (2009) 191, and references cited therein to earlier E176 work.
- [3] J.K. Ahn, et al., KEK E373 Collaboration, *Phys. Rev. C* 88 (2013) 014003, and references cited therein to earlier E373 work.
- [4] K. Nakazawa, et al., KEK E373 Collaboration, *Prog. Theor. Exp. Phys.* 2015 (2015) 033D02.
- [5] A. Gal, E.V. Hungerford, D.J. Millener, *Rev. Mod. Phys.* 88 (2016) 035004.
- [6] H. Ekawa, et al., J-PARC E07 Collaboration, *Prog. Theor. Exp. Phys.* 2019 (2019) 021D02.
- [7] S. Hayakawa, et al., J-PARC E07 Collaboration, *Phys. Rev. Lett.* 126 (2021) 062501.
- [8] M. Yoshimoto, et al., J-PARC E07 Collaboration, *Prog. Theor. Exp. Phys.* 2021 (2021) 073D02.
- [9] C.J. Batty, E. Friedman, A. Gal, *Phys. Rev. C* 59 (1999) 295.
- [10] E. Friedman, A. Gal, *Phys. Lett. B* 820 (2021) 136555; see also EPJ Web of Conferences 271 (2022) 03002.

- [11] D. Zhu, C.B. Dover, A. Gal, M. May, Phys. Rev. Lett. 67 (1991) 2268.
- [12] T. Koike, JPS Conf. Proc. 17 (2017) 033011.
- [13] M. Wang, W.J. Huang, F.G. Kondev, G. Audi, S. Naimi, *The AME2020 atomic mass evaluation*, Chin. Phys. C 45 (2021) 030003.
- [14] R.L. Workman, et al., Particle Data Group, Prog. Theor. Exp. Phys. 2022 (2022) 083C01.
- [15] T. Waas, M. Rho, W. Weise, Nucl. Phys. A 617 (1997) 449.
- [16] A. Gal, G. Toker, Y. Alexander, Ann. Phys. (NY) 137 (1981) 341.
- [17] K. Sasaki, et al. (HAL QCD Collaboration), Nucl. Phys. A 998 (2020) 121737.
- [18] J. Haidenbauer, U.-G. Meißner, Eur. Phys. J. A 55 (2019) 23.
- [19] D.J. Millener, in *Topics in Strangeness Nuclear Physics*, edited by P. Bydžovský, A. Gal, J. Mareš, Lect. Notes Phys. 724 (Springer, Heidelberg, 2007) pp. 31-79. The  $^1P_1$  phase relative to that of the other  $^{14}\text{N}$  wavefunction  $LS$  components in this reference is reversed here in Eq. (6) to enforce in our de-Shalit–Talmi [20] phase convention the check discussed in the text.
- [20] A. de-Shalit, I. Talmi, *Nuclear Shell Theory*, Academic Press (1963).
- [21] E. Friedman, A. Gal, *Constraints from  $\Lambda$  hypernuclei on the  $\Lambda NN$  content of the  $\Lambda$ -nucleus potential*, arXiv:2204.02264 and EPJ Web of Conferences 271 (2022) 06002.
- [22] M. Yamaguchi, K. Tominaga, Y. Yamamoto, T. Ueda, Prog. Theor. Phys. 105 (2001) 627.
- [23] J. Guo, X.-R. Zhou, H.-J. Schulze, Phys. Rev. C 104 (2021) L061307.